Advanced Composite Materials

ISSN: 0924-3046 (Print) 1568-5519 (Online) Journal homepage: http://www.tandfonline.com/loi/tacm20

A study on hardness of nickel-based cermet coatings composed of α-Al_2O_3 and TiO_2 nanoparticles

M.A. Farrokhzad & T.I. Khan

To cite this article: M.A. Farrokhzad & T.I. Khan (2015) A study on hardness of nickel-based cermet coatings composed of α-Al_2O_3 and TiO_2 nanoparticles, Advanced Composite Materials, 24:2, 141-159, DOI: 10.1080/09243046.2014.882537

To link to this article: http://dx.doi.org/10.1080/09243046.2014.882537

Advanced Composite Materials, 2015
Vol. 24, No. 2, 141–159, http://dx.doi.org/10.1080/09243046.2014.882537

A study on hardness of nickel-based cermet coatings composed of α-Al_2O_3 and TiO_2 nanoparticles

M.A. Farrokhzad* and T.I. Khan

Department of Mechanical and Manufacturing Engineer, The University of Calgary, 2500 University Drive NW, Calgary, Alberta, Canada T2N 1N4

(*Received 7 May 2013; accepted 9 January 2014*)

Nanostructured ceramic-metallic (cermet) coatings composed of one or two types of nanosized ceramic particles (α-Al_2O_3 and TiO_2) dispersed in a nickel matrix were produced using co-electrodeposition method. This research investigated the effects of alternating the concentration of ceramic particle in the electrolyte solution and applied current density on the microstructure, volume fraction of deposited particles in the nickel matrix and the microhardness of the coatings. The results showed that both α-Al_2O_3 and TiO_2 were uniformly distributed in the nickel matrix and the volume fraction of deposited ceramic particles in the matrix increased when the concentration of particles in the electrolyte was increased. Similarly, when higher current densities were applied, the volume fraction of deposited particle in the nickel matrix was increased to a maximum value of 12.6%. The results also showed that coatings with greater volume fraction of α-Al_2O_3 particles in the nickel matrix tend to have greater microhardness compared to the coatings with greater volume fraction of TiO_2 and when both type of ceramic particles were incorporated in the nickel matrix, the microhardness of coatings corresponded to the ratio of the ceramic particles concentration in the electrolyte solutions. The increase in microhardness of the cermet coatings produced in this study was attributed to a combined effect of dispersion-strengthening of ceramic particles in the Ni-matrix as well as grain refinement of the nickel matrix.

Keywords: co-electrodeposition; electrophoresis; nanostructured cermet coatings; dispersion-strengthening mechanism; microhardness

1. Introduction

Nanostructured ceramic-metallic (cermet) coatings are a group of engineered materials produced by incorporation of nanosized ceramic particles such as α-Al_2O_3 or TiO_2 particles into a metal matrix such as nickel. The cermet coatings can be produced using several coating techniques among which co-electrodeposition technique is being commonly used in the industry. Co-electrodeposition technique is a simple method and has several advantages among other coating techniques such as hot-dipping, vapour deposition and high velocity oxy-fuel coating spraying. The main benefits of using co-electrodeposition as compared to other techniques are: low production costs (material, energy and equipment), room temperature operation and practical capability to coat large and complex component geometries to a desired thickness.[1,2]

Due to the high demand from the oil and gas industry for using low-cost surface protection materials, in recent years there has been an increase in the number of

*Corresponding author. Email: mafarrok@ucalgary.ca

industrial applications where cermet coatings were used to enhance the surface hardness and improve the wear and corrosion resistance of the mechanical components.[3,4] When hard nanosized ceramic particles such as alumina (α-Al_2O_3: 2000–2600 HV.) and titania (TiO_2: 880–1121 HV.) are incorporated in a corrosion resistant metal like nickel, the produced cermet material shows higher microhardness values compared to the pure or alloyed form of nickel.[5–7] Research has shown that the mechanical properties of nickel-based cermet coatings are greatly influenced by two factors; firstly, the type and volume fraction of deposited ceramic particles in the nickel matrix, and secondly, the average grain size of the nickel matrix.[8] Researchers have incorporated α-Al_2O_3 and TiO_2 particles in the nickel matrix for different reasons; for example, α-Al_2O_3 is usually used to improve the hardness whereas TiO_2 has been used to improve the cohesion of the formed oxide film to the coating surface for high-temperature applications. It should be noted that the presence of titanium in nickel results in internal formation of $NiTiO_3$ (perovskite) in the nickel matrix at elevated temperatures. The formation of $NiTiO_3$ near the surface of the coatings has a beneficial effect on strengthening the oxide scale which can prevent scale buckling on the surface of the coatings. TiO_2 usually forms a perovskite structure of $NiTiO_3$ with nickel at elevated temperatures of over 500 °C.

The general approach in controlling and enhancing the mechanical properties of cermet coatings are done by optimization of electrodeposition parameters such as ceramic particle size, concentration of particles in the electrolyte solution and controlling the applied current density. A higher concentration of ceramic particles in the electrolyte solution will increase their deposition rate in the matrix as a result of increasing the availability of particles at the deposition sites.[9] Also, the nanosized particles are more prone to stay suspended in the electrolyte solution compared to microsized particles (due to mass-surface area ratio) and as a result, the nanosized particles provide a more uniform and homogenous distribution of deposited particles in the nickel matrix.[8] The deposition rates for both nickel cations and ceramic particles are also dependent on the applied current density.[10] An increase in the magnitude of applied current density will increase the volume fraction of deposited ceramic particles in the metallic matrix and will decrease the grain size of the metallic matrix.[11]

The co-electrodeposition of cermet coatings consists of two separate electrochemical reactions that occur simultaneously in the electrolyte solution and on the surface of the substrate; (1) the electrocrystallization of metallic matrix and (2) electrophoresis of ceramic particles into the metallic matrix. The electrocrystallization of the metallic matrix have been extensively studied in the past by Bockris and Razumney [12] and Walsh and Herron [13] and it has been recently revived through the work of Qu et al. [14], Ruan and Schuh [15], Feng et al. [16] and Kim et al. [17]. During the electrocrystallization of the matrix, the charged metallic cations (separated from the anode) migrate through the electrolyte solution and then become deposited on the surface of the substrate. Meanwhile, in electrophoretic deposition of particles, the suspended ceramic particles in the electrolyte solution become electrostatically charged and then under electrostatic attraction migrate towards the deposition sites on the surface of the substrate. Electrophoretic migration of nanosized ceramic particles is controlled by the electrophoretic velocity which is a function of the electric field between the anode and the cathode in the solution, and the zeta potential between the particles and the electrolyte solution. Bund and Thieming [18,19] have shown that for the pH range of 4.0–4.2 in nickel sulphate and nickel chloride solutions (Watt's solution), the zeta potential remains unchanged, therefore this pH range was selected for the electrolyte solution used in this study.

The mechanical properties of cermet coatings are also affected by the quantity of deposited ceramic particles in the nickel matrix. The improved microhardness of materials can be attributed to both the dispersion-strengthening effect explained by *Orowan* mechanism, and grain size refinement explained by *Hall–Petch* mechanism.[20] Erb [11] has studied the changes in mechanical properties of nanocrystalline nickel and has shown that the mechanical and physical properties of cermet coatings such as wear resistance, strength, ductility and hardness can be significantly improved by grain refinement of the nickel matrix, however some other mechanical properties such as *Young's* modulus, adhesion to substrate and thermal expansion coefficient remain unchanged. Theming and Bund [20] and Sedighi et al. [21] have shown that the presence of nanosized ceramic particles at the deposition sites can influence the crystallization of the matrix by disturbing the normal growth of nickel crystals whilst forming new nucleation sites around the deposited particles. In addition, Low et al. [22] have also shown that the change in the crystalline growth of a metal deposit can result in an increase in the number of defects in the matrix crystal structure and as a result, a greater microhardness could be expected for cermet coatings when compared to pure metal coatings. The hardness of cermet coatings can also be increased as a result of dispersion-strengthening mechanism caused by the presence of ceramic particles in the matrix. Dispersion-strengthening mechanism also explains that in addition to the mechanical strength of the dispersed particles, their size, volume fraction in the matrix and distribution pattern can also influence the mechanical properties of the cermet coating.[23] In this case, it is believed that the matrix carries the compressive force while the dispersed particles obstruct the dislocation motion. It also should be noted that based on results from Gül et al. [9], when the volume fraction of dispersed particles in the matrix exceeds 20%, particle-strengthening mechanism (instead of dispersion-strengthening) becomes the dominating hardening process.

In this study, attempts have been made to develop novel cermet coatings composed of one or two types of particle dispersions (α-Al_2O_3 and TiO_2) incorporated in a nickel matrix. For naming purposes, these new coatings are called "double-ceramics" as compared to the conventional "single-ceramic" cermet coatings composed of only one of the α-Al_2O_3 or TiO_2 particles. Research has shown that adding α-Al_2O_3 particles in the nickel matrix can improve the hardness whereas adding TiO_2 particles in the nickel matrix can improve the high-temperature oxidation resistance of the cermet coatings. However, the literature review shows that very little experiments have been conducted on microstructure and microhardness of double-ceramics cermet coatings. The objectives of this research focused on the effects of alternating concentrations of ceramic particles in the electrolyte solutions and applied current density on deposited volume fraction of particles in the matrix and the microhardness of the cermet coatings. The co-electrodeposition of coatings was conduced on AISI-1018 carbon steel specimens in a standard *Watt's* electrolyte solution composed of one or two ceramic particles and with respect to two molar concentration of particles the solution (0.25 and 0.5 M) and applied current density of 1, 2 and 3 A/dm^2. The microstructure features of coatings were analysed using scanning electron microscopy (SEM) and wavelength dispersive spectroscopy (WDS) element mapping techniques. The volume fraction of particles in the nickel matrix was calculated using *Image J* software. The microhardness values for the coatings were measured and the results compared with respect to the particle concentration in the electrolyte solution and applied current density.

2. Experimental procedure

2.1. Materials

This study used two types of nanosized powders; aluminium III oxide (aka alumina or α-Al_2O_3) and titanium oxide II (aka titania or TiO_2) purchased from M K Impex Corp. Ltd. The purity for α-Al_2O_3 was 99.95% (with traces of Na: 300 ppm, Si: 3.5 ppm, Ca: 1.6 ppm, Fe: 0.2 ppm, and Co: 0.8 ppm). The purity for TiO_2 was 98% (with traces of Al: 20 ppm, Ca: 75 ppm, Mg: 65 ppm, Nb: 119 ppm, S: 165 ppm and Si: 102 ppm). The average grain size was 20 nm for α-Al_2O_3 and 50 nm for TiO_2. The anode was made of a high purity nickel bar (99.9%). The substrate material was made from hot-rolled AISI-1018 carbon steel bars and the specimens for co-electrodeposition were cut in a rectangular shape (length: 20 mm, width: 12.7 mm and thickness: 6.5 mm) using a band saw. The mill scale was removed by mechanical cleaning and the surface was prepared to a 600 grit finish. The surfaces were then cleaned in alkaline solutions (E-Kleen 102-E™ and E-Kleen 129-L™) and finally an acidic solution (acid pickling with 31% HCl) was used to remove any remaining grease or other contaminates.

2.2. Microstructural characterization

For the grain-size analysis of the powders and nickel matrix, a *Tecani F20-200kV* (the Netherlands) transmission electron microscope (TEM) in bright field (BF) mode was used. A *JSM-8200 JEOL* micro-probe (Tokyo, Japan) SEM in the back-scattered electron mode (BSE) was used for the images of the cross-sections of the coatings. The element maps of the coatings were also produced using the WDS of the same *JSM-8200 JEOL* micro-probe.

2.3. Co-electrodeposition

The standard *Watt's* bath formula was used for the chemical composition of the electrolyte solution and the concentrations of ceramic particles in the electrolyte solution were obtained from previous research.[10,17,24] The pH of the electrolyte solutions was 4.0–4.2, and the temperature of the electrolyte solution was kept between 50 and 55 °C. Two groups of cermet coatings were co-electrodeposited; the first group (or single-ceramic cermet coatings) was composed of only one ceramic powder (α-Al_2O_3 or TiO_2) and the second group (or double-ceramics cermet coatings) was composed of the two ceramic powders. The electrolyte solutions for double-ceramics cermet coatings were also composed of two mixtures of ceramic powders which were called; A and B coatings. The "A" mixtures (A1 for 0.5 M and A2 for 0.25 M total concentration of particles in electrolyte) were made in electrolyte solutions containing an equal ratio of both ceramics (50% of α-Al_2O_3 and 50% of TiO_2). The "B" mixtures (B1 for 0.5 M and B2 for 0.25 M total concentration of particles in electrolyte) were made in electrolyte solutions containing a ratio of 75% of α-Al_2O_3 to 25% of TiO_2. The coatings classification and the compositions of the electrolyte bath solutions are summarized in Table 1. The pure Ni coating was also electrodeposited for reference.

The anode was made of commercial high purity nickel (99.9%). The coatings were produced using a DC set-up. The applied current densities were 1, 2 and 3 A/dm^2 for a time period of 60 min. SEM (*JOEL JXA-8200*) was used to measure the average electroplated thickness. The produced average thickness was measured to be 40 ± 5 μm.

Table 1. Type and concentration of ceramic powders in electrolyte solutions.

Coatings	Molar Concentration	Particles in electrolyte [gr/lit]	Stirring Speed [rpm]	Electrolyte Composition
Pure Ni	n.a.	n.a.	100	
Ni+Al_2O_3	0.5 M	α-Al_2O_3: 51	400	
Ni+Al_2O_3	0.25 M	α-Al_2O_3: 25.5	400	Standard *Watt*'s bath solution:
Ni+TiO_2	0.5 M	TiO_2: 40	300	1 M: $NiSO_4.6H_2O$ (Nickel Sulphate Hexahydrate)
Ni+TiO_2	0.25 M	TiO_2: 20	300	0.2 M: $NiCl_2.6H_2O$ (Nickel Chloride Hexahydrate)
A1	Total of 0.5 M:	α-Al_2O_3: 25.5	350	0.5 M: H_3BO_3 (Boric acid), dissolved in distilled water (H_2O).
	α-Al_2O_3: 0.25 M TiO_2: 0.25 M	TiO_2: 20		
B1	Total of 0.5 M: α-Al_2O_3: 0.375 M TiO_2: 0.125 M	α-Al_2O_3: 38.25 TiO_2: 10	380	
A2	Total of 0.25 M: α-Al_2O_3: 0.125 M TiO_2: 0.125 M	α-Al_2O_3: 12.75 TiO_2: 10	320	
B2	Total of 0.25 M: α-Al_2O_3: 0.1875 M TiO_2: 0.0625 M	α-Al_2O_3: 19.2 TiO_2: 5	340	

2.4. *Microhardness*

Prior to microhardness tests, the surfaces of all coated specimens were prepared by using standard metallurgical surface preparation techniques with a final polish using 0.25 μm diamond paste. The microhardness tests were conducted across the transverse sections of the coating using a *Leitz Miniload-2* microhardness Vickers tester equipped with a diamond pyramid indenter operating under 25 g load. The number of indentations follows ASTM E384-10 requiring a minimum of 10 indentations per coating. In this research, 25 indentations were made for each coating and the average microhardness values were calculated using the following equation:

$$Hv = 1854.4\frac{P}{d^2} \tag{1}$$

where P is gram-force (gf) and d is the diagonal of indentation in micrometres.

3. Results and discussion

3.1. *The structure of nanosized ceramic powders*

Field emission scanning electron microscopy (FE-SEM) and TEM confirmed the as-received powder average grain size. Figure 1 represents the FE-SEM and TEM images of nanosized α-Al_2O_3 and TiO_2 ceramic powders. A close observation of the TEM images in Figure 1 showed the agglomeration of particles and formation of a

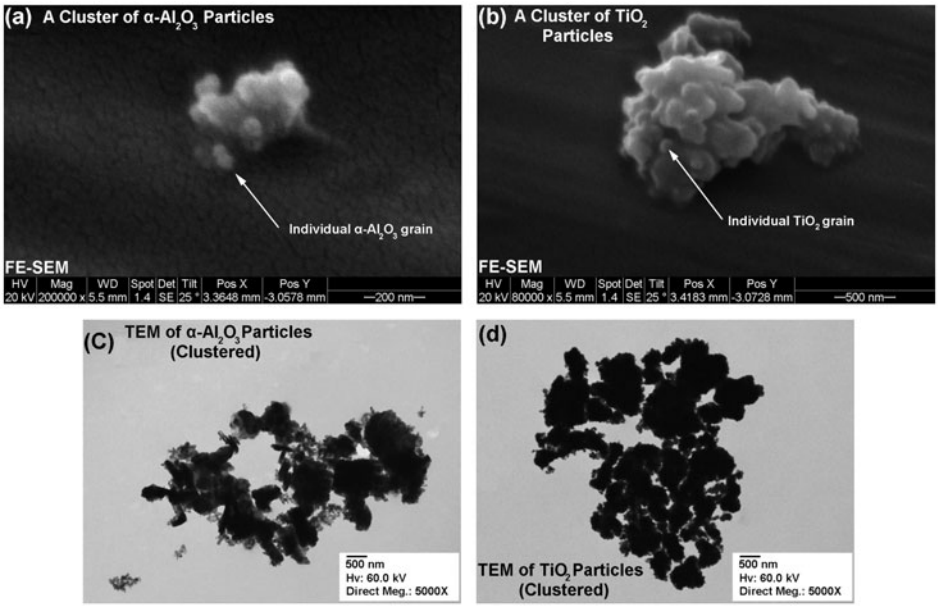

Figure 1. FE-SEM and BF TEM images of α-Al_2O_3 (a and c) and TiO_2 (b and d) powders.

large cluster. The WDS element mapping of the cross-section of the coatings (see Figure 2) also revealed that the size of some of the dispersed particles was greater than the as-received grain size, which indicated that large clustered particles from the electrodeposition electrolyte solution were deposited in the nickel matrix during the co-electrodeposition process.

Figure 2 images (element maps) are from the nickel-based cermet coatings with α-Al_2O_3 and TiO_2 particles dispersed in the nickel matrix. It should be noted that colours in Figure 2(b–d) images are element distribution of the Figure 2(a) and they should not be translated as different images. The image shown in Figure 2(a) is the surface of the coating; the grey shade in the background is indeed the nickel matrix and the dark spots are dispersed α-Al_2O_3 and TiO_2 particles. The bright colours in Figures 2(b–d) images correspond to the respective elements and the dark colour corresponds to the lack of the detecting elements at the location. For instance, the bright colour (yellow background) in Figure 2(b) corresponds to the large quantity of nickel where as in Figure 2(c) and (d), the bright spots correspond to α-Al_2O_3 particles (Figure 2(c)) and TiO_2 particles (Figure 2(d)). The blue background colour in Figure 2(c) and (d) correspond to the lack of α-Al_2O_3 and TiO_2 particles (hence, presence of nickel matrix). The colour scale for the element maps displays the local X-ray intensity (measured as [counts/μA.ms]) at the given locations. The X-ray intensity of each element can be correlated to relative concentration (mass%) of the selected elements on the maps. The conversion of X-ray intensity of an element to its relative mass% concentration (C') can be done using *Castaing's* approximation ($C' \approx \frac{I_{sp}}{I_{st}} C_{st}$) where I_{sp} and I_{st} are the intensity measured from the specimen and the standard sample, respectively, and C_{st} is the concentration of the element in a known standard sample. The values for the intensity (I_{st}) and concentration (C_{st}) for the standard sample can be obtained from a known pure form of the element. It should be emphasized that the

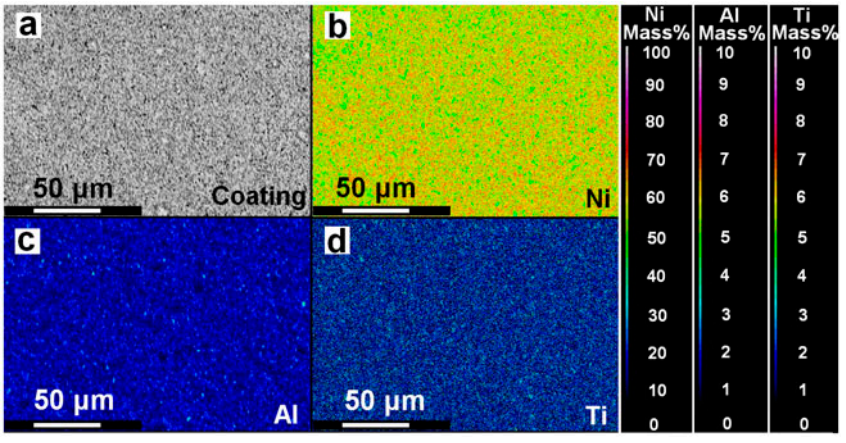

Figure 2. X-ray element mapping of A1 coating; surface of coating (a), nickel (b), aluminium (c) and titanium (d).

measured values for the relative mass% concentration of each element in the map should be considered as an approximation because a variety of other parameters such as spectrometer arrangement, age of spectrometer filament, beam intensity and so on can affect the accuracy of the measured X-ray intensity.

3.2. Characterization of coatings

The appearances and morphology of the coatings deposited using a current density of 1, 2 and 3 A/dm^2 were, in general, similar and a uniform distribution of α-Al_2O_3 and TiO_2 particles in the nickel matrix was produced for all the coatings. The cross-section of the A1 cermet coatings produced with a current density of 2 A/dm^2 is displayed in Figure 3. The thickness of the coated films was measured from the cross-section of the coated specimens and observed to vary with current density. In general, the thickness of the coated films increased with an increase in the current density and a coating thickness of 40–45 µm was measured for the deposited coatings at a current density range of 1–3 A/dm^2.

The randomly distributed dark dispersions in the SEM images of the cross-section of the coatings are the dispersed particles in the Ni matrix (the brighter gray region)

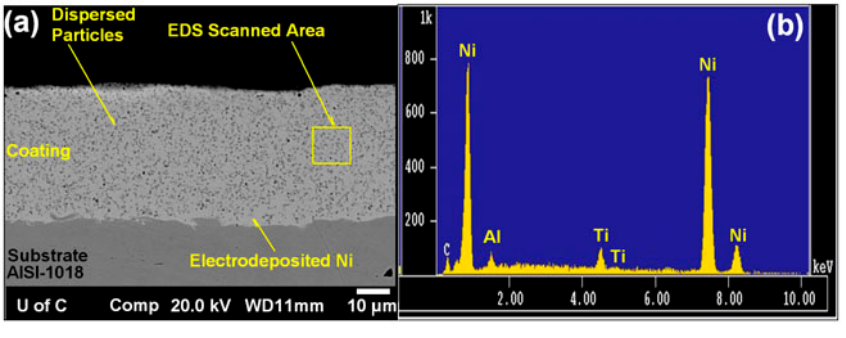

Figure 3. SEM image of cross-section (a) and WDS compositional analysis and (b) of the A1 cermet coating.

and the darker grey region in the image is the carbon steel (AISI-1018) substrate. The WDS compositional analysis taken from these dispersions showed that they are rich in aluminium and titanium. The WDS element mapping of the cross-section of the coatings with respect to nickel (Ni), aluminium (Al) and titanium (Ti) elements (shown in Figure 2) also indicated a uniform distribution of dispersed particles in the nickel matrix.

3.2. *Dispersed particle contents*

Mathematical models for correlating the content of particles in the matrix to the electrodeposition parameters still needs to be developed,[22] however, there is a significant amount of published experimental work that can be used for estimating the particle content with respect to the electrodeposition parameters. Table 2 is a summary of recent investigations for measuring the particle content for electrodeposition of $Ni + Al_2O_3$ and $Ni + TiO_2$ coatings similar to the co-electrodeposition conditions used in this research. For the majority of these studies, the particle volume fraction in the Ni matrix increases by increasing current density and concentration of particles in the electrolyte solutions, however there are some exceptions to this rule. The measured values for particle volume fraction in the Ni matrix for the coatings produced for this research (see Table 3) were found to be close to the values measured by Marikkannu [25], Gül et al. [9], Chen et al. [26] and Thiemig et al. [27,28] for $Ni + Al_2O_3$ coatings and Abdel and Hassan [29], Spanou et al. [30] and Parida et al. [31] for $Ni + TiO_2$ coatings.

For this research, a method described by Parida et al. [31] was used (as shown in Figure 4) to measure the particle volume fraction and size in the nickel matrix using "*Image J*" software program and the results of the effect of applied current and time of electrodeposition on the concentration of dispersed particles in the nickel matrix is shown in Table 3.

The volume fractions represented in Table 3 show that the concentration of co-deposited particles increased with an increase current density from 1 to 3 A/dm^2; however, this increase is within a 2% range. Several researchers have investigated the effect of current density on the electrodeposition of $Ni + Al_2O_3$ and $Ni + TiO_2$ coatings in the past. The general observation is that the volume fraction of dispersion in the metallic matrix increases initially with the increase in current density magnitude to the maximum at 3 A/dm^2 and then the amount of dispersed α-Al_2O_3 particles remains less affected beyond this current density.[8,9,21,32,33]

3.3. *Microhardness of coatings*

Figure 5(a) is the SEM images of an array of microhardness indentations on the coating cross-section and Figure 5(b) and (c) are the plan-view SEM and BSE images of the microindentations.

The microhardness measurements are provided in Figure 6 for the single-ceramic and Figure 7 for double-ceramics cermet coatings as a function of applied current density. The microhardness for the pure Ni coating is also added for comparison purposes. The graphs shown in Figures 6 and 7 also provide the mean and the error bars of the microhardness measurements for the coatings.

Table 2. Reported concentrations of α-Al_2O_3 and TiO_2 into the electrolyte and Ni matrix produced by co-electrodeposition.

Coating	Research by	Current Density Range [A/dm^2]	pH	Particle Size Range [nm]	Nanoparticle Concentration In Solution [gL^{-1}]	Nanoparticle Concentration Volume Fraction in Matrix (Vol. %)	Notes from References
Ni+Al_2O_3	Kuo et al. [24]	3.0	4.0	80	5	8.37–24.65	Alternating concentration of Ni^{2+} in solution
	Marikkannu [25]	2.0–5.0	4.0	20–40	25	4.2	Study of molar concentration and current density
					50	5.3	
					75	6.7	
					100	7.5	
					125	7.2	
	Low et al. [22]	5.0–25.0	4.0	600–800	75	Approx. 7–20	From Figure 3 [22]
					150	Approx. 18–34	
					225	Approx. 27–39	
	Chen et al. [26]	3.0	4.0	800	20	8.6–14.7	Alternating surfactant in the electrolyte
	Gül et al. 2009 [9]	1, 3, 6, 9	4.0	80	5, 10, 20, 30	4.1(1 A/dm^2)	Constant 20 gL^{-1}
						8.3(3 A/dm^2)	From Figure 6 [9]
						8.2 (6 A/dm^2)	
						8.7 (9 A/dm^2)	
						4.0 (5 gL^{-1})	Constant 3 A/dm^2
						6.0 (10 gL^{-1})	From Figure 4 [9]
						8.0(20 gL^{-1})	
						11.0% (30 gL^{-1})	
	Thiemig et al. [27,28]	5, 10, 15, 20	4.3	13–50	10	6.0–8.0	From Figure 3 [27,28]
					30	8.0–10.0	
					60	7.0–9.0	
					90	8.0–10.0	
					120	12	
	Saha et al. [8]	0.5–3.0	4.0	50	50	4.3	From Figure 3 [8]
Ni+TiO_2	Low et al. [22]	6.0–7.0	3.0	12	0–200	0–11.0	From Table 4 [22]

(*Continued*)

Table 2. (*Continued*).

Coating	Research by	Current Density Range [A/dm^2]	pH	Particle Size Range [nm]	Nanoparticle Concentration In Solution [gL^{-1}]	Nanoparticle Concentration Volume Fraction in Matrix (Vol. %)	Notes from References
		2.0		20	10–120	0–20.0	
	Abdel et al. [29]	1.0, 2.0, 3.0	5.0	25	0.5–5.0	6.0 (1 A/dm$^{2)}$ 8.0 (2 A/dm^2) 8.5 (3 A/dm^2)	From Figure 1 [29]
	Spanou et al. [30]	0.4–40.0	4.4	20–21	20 50 100	4.5 5.5 7.0	From Figure 6 [30]
	Parida et al. [31]	5.0	4.0	30	5–15	5.0–7.0	From Figure 7 [31] Alternating surfactant

Table 3. Particle count volume fraction and average deposited particle size for co-electrodeposited coatings.

Coating	Molar Concentration	Study of Applied Current Density		
		1 A/dm^2	2 A/dm^2	3 A/dm^2
Ni + Al_2O_3	0.5 M	9.3%	8.9%	10.0%
		880 nm	810 nm	930 nm
	0.25 M	8.8%	8.0%	8.2%
		940 nm	790 nm	580 nm
Ni + TiO_2	0.5 M	10.8%	12.6%	11.8%
		920 nm	840 nm	690 nm
	0.25 M	9.2%	9.7%	10.8%
		1010 nm	830 nm	670 nm
A	A1	9.9%	11.8%	10.8%
		690 nm	540 nm	820 nm
	A2	8.9%	9.5%	9.9%
		840 nm	910 nm	940 nm
B	B1	9.8%	9.2%	10.5%
		690 nm	630 nm	910 nm
	B2	8.5%	8.9%	9.3%
		520 nm	720 nm	650 nm

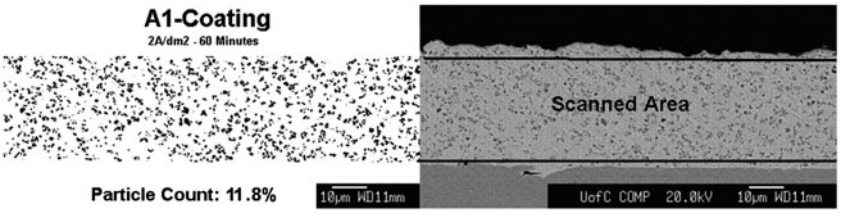

Figure 4. Particle count on A1 coating using *Image J* software program.

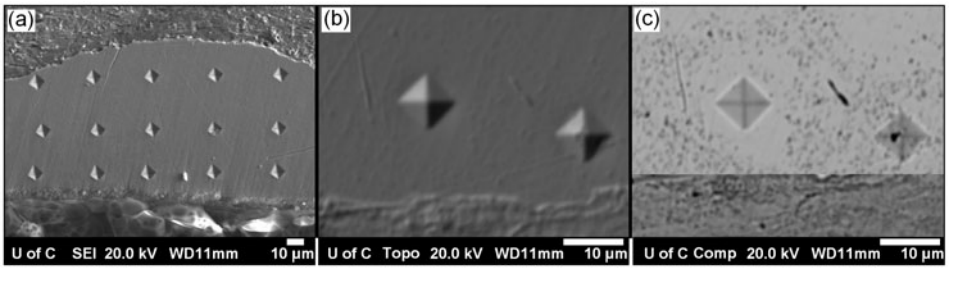

Figure 5. An array of micro-indentation on the coating thickness (a), top-view SEM image of micro-indentation (b) and backscattered secondary beam SEM of micro-indentation and (c) showing the diagonal lengths used for measuring hardness.

3.3.1. Effects of dispersed particles on the hardness of the nickel matrix

The cermet coatings produced for this research exhibit greater microhardness compared to pure Ni coatings produced with the same applied current densities (Figures 6 and 7).

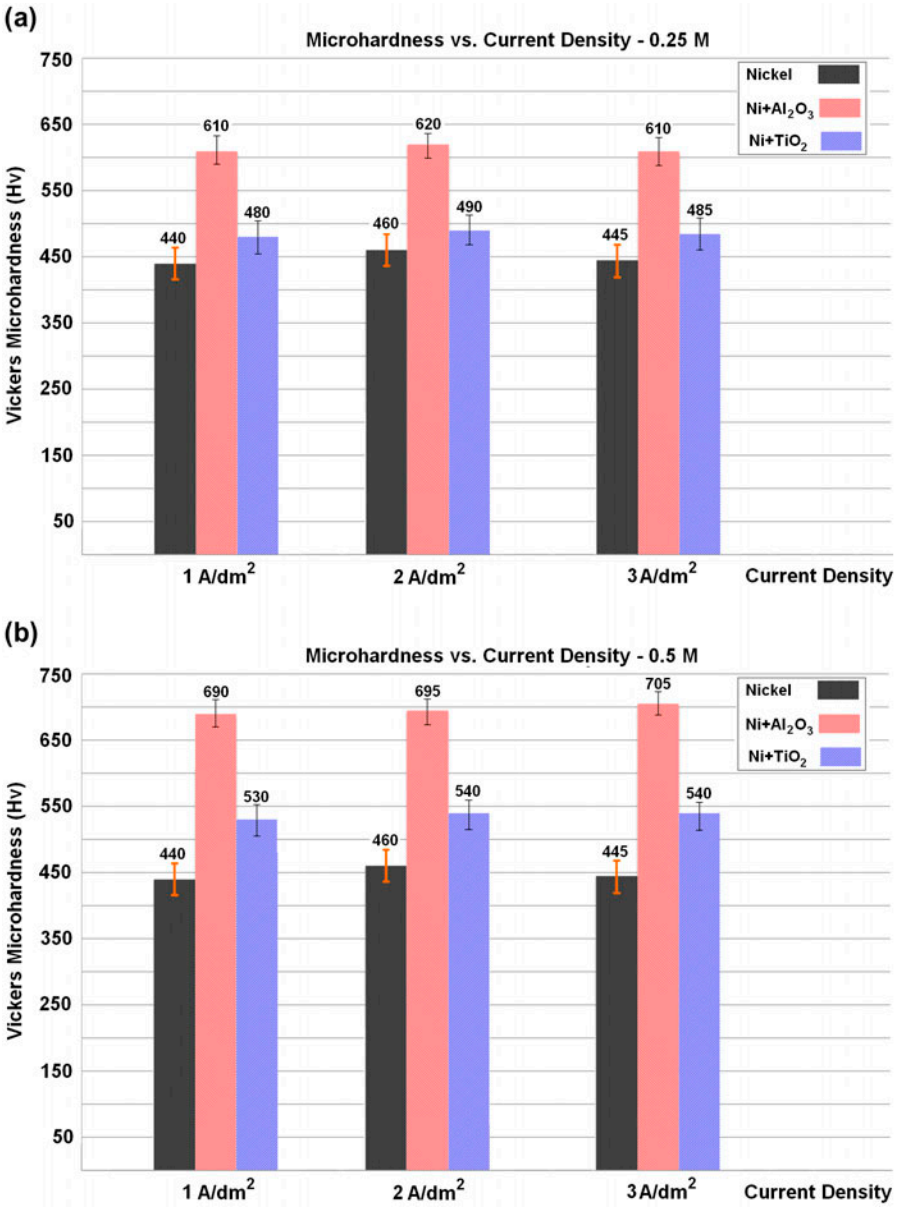

Figure 6. Microhardness (Vickers) measurements for pure Ni coating and single-ceramic cermet coatings as a function of applied current density for both 0.25 M (a) and 0.5 M and (b) electrolyte solutions.

These results were in agreement with the earlier work by Saha and Khan [8] and Gül et al. [9]. The reinforcement of α-Al_2O_3 and TiO_2 particles dispersed in the nickel matrix can increase the hardness by two possible hardening mechanisms; firstly, by the dispersion-strengthening of the matrix as a result of an increase in particle volume fraction in the matrix. Secondly, the dispersion of nanosized particles can also help grain size refinement (by reducing the average grain size in the nickel matrix) and as a

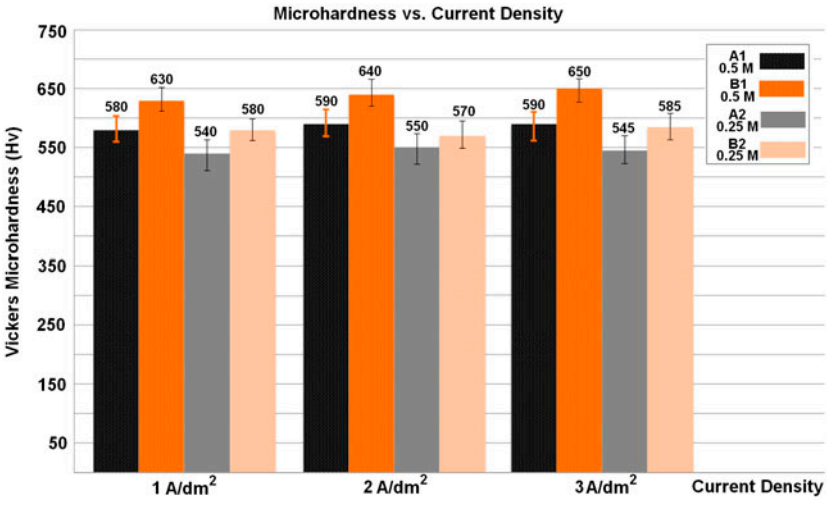

Figure 7. Microhardness (Vickers) measurements for double-ceramics cermet coatings as a function of applied current density for both 0.25 M and 0.5 M electrolyte solutions.

result, an increase in the hardness of the matrix can be expected (*Hall–Petch* effect). Increasing the magnitude of applied current density and particle concentration in the electrolyte solution can increase the deposition rate of ceramic particle in the matrix and at the same time, it can reduce the average size of nickel grains.[21,32,34–36] Gül et al. [9] have discussed three separate mechanisms that can account for increasing the hardness for cermet coatings: (1) grain refining, (2) dispersion-strengthening and (3) particle-strengthening, when the volume fraction of dispersed particles is less than 15% and their size remains below 1000 nm, "dispersion-strengthening" is the main contributor to the hardness of cermet coatings. The "particle-strengthening" occurs when the volume fraction of dispersed particles is greater than 20%.[9]

Figures 6 and 7 also illustrate significant differences in measured values of microhardness with respect to the type of ceramic particle deposited in the nickel matrix. The greater microhardness values for cermet coatings can be attributed to their greater compressive strengths and modulus of elasticity as compared to pure Ni and can be explained based on the "rule of mixture" for composite materials. The rule of mixture for a composite material states that the elastic mechanical properties of a composite material can be formulated on the basis of volume fraction and the elastic properties of the individual constituents expressed by [37–40]:

$$\sigma_{\text{Comp.}} = \sigma_m V_m + \sigma_c V_c = \sigma_m (1 - V_c) + \sigma_c V_c \tag{2}$$

$$E_{\text{Comp.}} = E_m V_m + E_c V_c = E_m (1 - V_c) + E_c V_c \tag{3}$$

where $\sigma_{\text{Comp.}}$, σ_m and σ_c are, respectively, the compressive strengths for cermet (composite) material, the matrix material and the ceramic particles. Similarly, $E_{\text{Comp.}}$, E_m and E_c are the modulus of elasticity for the same materials. V_c is the volume fraction of the dispersed ceramic particles in the matrix material and V_m is the volume fraction of the matrix material ($V_c + V_m = 1$). The mechanical properties and Vickers hardness values for the ceramics particles used in this study are provided in Table 4.

Table 4. Mechanical properties of α-Al_2O_3 and TiO_2 particles.

	α-Al_2O_3	TiO_2
Compressive strength	2.945 GPa at 25 °C	680 MPa at 25 °C
Young modulus	344–408 GPa at 25 °C	282–431 GPa at 25 °C
Hardness (Vickers)	2600 HV.	880–1121 HV.

The Ni + Al_2O_3 coating shows a significantly greater hardness value compared to the Ni + TiO_2 coating and this difference can be attributed to the greater compressive strength and modulus of elasticity of α-Al_2O_3 particles compared to TiO_2 particles.

The dispersion of hard ceramic particles in the nickel matrix can reinforce and enhance the compression strength of the nickel matrix. As expected, the dispersion of α-Al_2O_3 provides greater yield strength as compare to the dispersion of TiO_2 to the coatings, which can be attributed to the greater compressive strength values for α-Al_2O_3 to TiO_2 particles. Comparing the microhardness of A1, B1, A2 and B2 coatings (Figure 7) to the microhardness of Ni + Al_2O_3 and Ni + TiO_2 coatings made with similar molar concentration of particles in the electrolyte solution (Figure 6) reveals that the hardness of the double-ceramics coatings are measured somewhere between the hardness of Ni + Al_2O_3 and the hardness of Ni + TiO_2 coatings. B1 and B2 coatings show greater hardness values compared to A1 and A2 coatings and this can be attributed to the greater availability of α-Al_2O_3 particles (75%) in the electrolyte solution compared to the TiO_2 particles (25%) and also to the greater compressive strength and modulus of elasticity of α-Al_2O_3 particles compared to the TiO_2 particles. It also should be mentioned that using TiO_2 improves the mechanical properties of cermet coating at elevated temperatures. TiO_2 usually forms a perovskite structure of $NiTiO_3$ at elevated temperatures over 500 °C which has a beneficiary effect of preventing the buckling of the oxide layer formed on the surface of the coatings at elevated temperature applications.[48]

3.3.2. *Effects of particle concentration in electrolyte solution on hardness*

The microhardness results showed that coatings made from a 0.5 M electrolyte solution had greater hardness values compared to coatings made from a 0.25 M electrolyte solution (see Figures 6 and 7). This change in hardness values as a function of molar concentration can be correlated to the greater quantity of ceramic particles available in the 0.5 M solution compared to the 0.25 M solutions. The greater quantity of ceramic particles in solution increases the probability of attraction and trapping of the particles into the Ni-matrix during the electrophoresis process, and a greater volume fraction of dispersion in the Ni-matrix can be expected. Erler et al. [33] have studied nanocrystalline Ni cermet coatings and have shown that the hardness of the cermet coatings can be improved by varying the type, size, amount and distribution of the incorporated particles. The greater volume fraction of dispersion particles gives rise to the higher compressive strength (Equations (2) and (3)) and as a result, greater hardness values can be expected for the coatings made in 0.5 M solutions compared to the 0.25 M solutions.

3.3.3. *Effects of current density on hardness*

An alternation in the applied current density can affect the attraction rate of ceramic particles into the matrix and at the same time it can influence the adsorption rate for

metallic cations into the matrix. Gül et al. [9] have studied the effects of concentration on the hardness of $Ni + Al_2O_3$ and have shown that microhardness measurements of cermet coatings are increased when the applied current density and the concentration of electrolyte solutions were increased. An increase in the attraction rate of ceramic particles into the nickel matrix will increase their volume fraction of ceramic particles (V_c) and higher hardness values can be expected. Additionally, the increase in the magnitude of applied current density also increases the rate of adsorption of nickel cations into nickel matrix which results in a higher volume fraction for nickel matrix (V_m). Since nickel grains have significantly lower hardness values compared to ceramic particles (compare Figure 8 to Table 4), this increase in the amount of attracted nickel cations into the nickel matrix can lower the overall hardness of coatings which is also affected by increasing the attraction rate of ceramic particles into the matrix. An increase in the ratio between the volume fraction of ceramic particles to the volume fraction of the nickel matrix (V_c/V_m) is the determining factor in increasing the hardness of the cermet coatings. Additionally, Bund and Thiemig [18,19] have discussed that the current density influences the microstructure (as well as the volume fraction of dispersed particles) in the matrix, which in return affects hardness of the coatings. An increase in hardness can be expected with an increase in the current density because of the decrease in grain size of the depositing nickel grains.[41]

3.3.4. *Hall–Petch behaviour of nickel grains*

The presence of dispersed nanosized particles at the electrodepositing sites inhibits the nickel grain growth and thus it leads to a smaller nickel crystallite structure which can cause an increase in the microhardness of the coatings.[19] Zimmerman et al. [42] have discussed that the restrictions on dislocation generation and mobility caused by ultrafine grain size can potentially be the dominant factor in increasing the hardness of cermet materials as followed by the *Hall–Petch* equations. The relationship between the hardness and the tensile strength of the nickel matrix follows the *Hall–Petch* relationship,

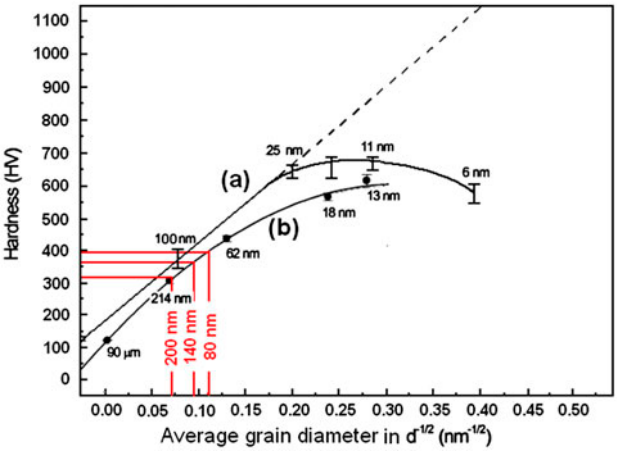

Figure 8. Hall–Petch deviation for electrodeposited Ni (a) produced by Erb [11] and the hardness values for grain sizes measured in this research (80, 140 and 200 nm) projected on the graph (b) produced by Jeong et al. [47].

which correlates the compressive strength and hardness of the metal to the average grain size of the metal and can be expressed by [43]:

$$\sigma_{TS} = \sigma_o + k_{TS} d^{-1/2} \tag{4}$$

$$H = H_o + K_H d^{-1/2} \tag{5}$$

where σ_o and H_o are lattice related constants (usually the compressive strength and hardness of the material measured in single-crystal form), K_{TS} and K_H are material-dependent constants and d is average grain size. The ASTM E 112, "Standard Test Method for Determining Average Grain Size" provides details for estimating the grain size based on the metallographic analysis of the materials. From Equations (4) and (5) it is expected that the nickel matrix with smaller grains to have greater compressive strength and hardness compared to a nickel matrix with larger grains.[43,44] However, it should be noted that some materials (i.e. nanocrystalline electrodeposited nickel) can also show deviations from the *Hall–Petch* behaviour by having a transition from grain-size strengthening to grain-size softening at some specific grain sizes. El-Sherik and Erb et al. have discussed that nanocrystalline electrodeposited nickel shows a continuous increase in hardness with decreasing grain size (regular *Hall–Petch* behaviour) but

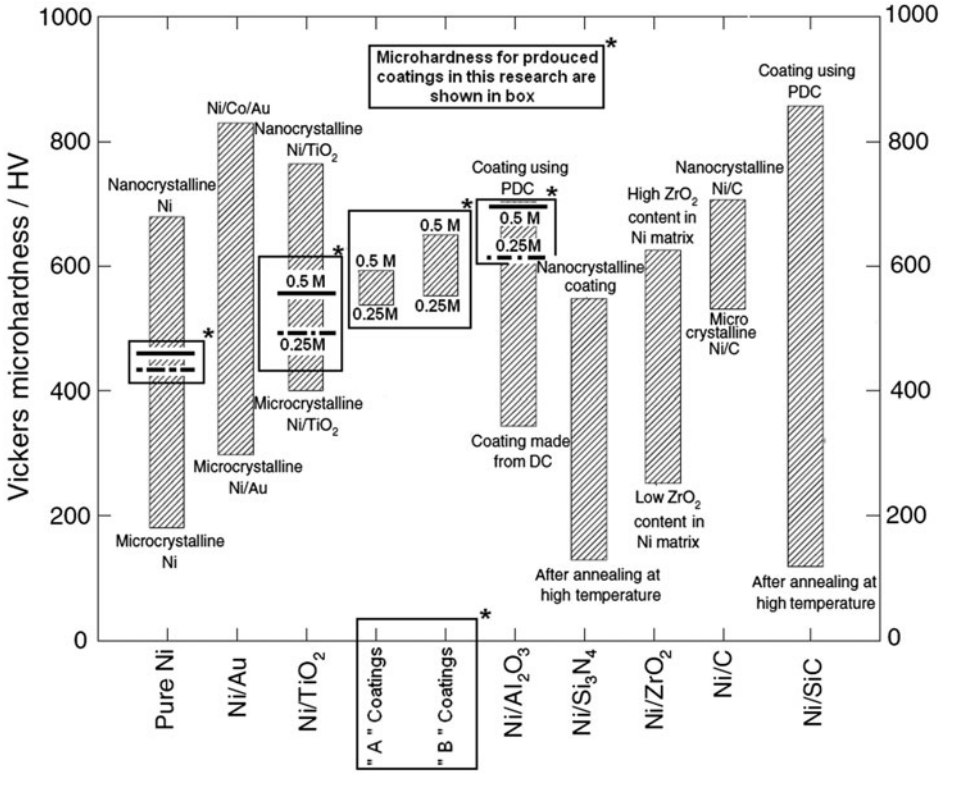

Figure 9. Relative microhardness values for coatings produced in this research as compared to microhardness of several other types of cermet coatings from the literature reported by Low et al. [22].

for grain sizes less than 30 nm a clear deviation from *Hall–Petch* (softening or inverse *Hall–Petch* behaviour) can be observed (see Figure 8).[11,45,46]

There are several mechanisms that can explain the inverse *Hall–Petch* behaviour including; the effects of triple junction on the dislocations (at the intersection line of three or more grain boundaries), diffusional creep, texture effects and a decrease in interfacial excess volume.[42] However, since the measured grain sizes for electrodeposited nickel coatings in this research are measured to be 80–200 nm (with an average of 140 nm), the inverse *Hall–Petch* behaviour is less likely to have an impact on the material in this research and *Hall–Petch* formulas can be used for explaining the effect of grain size on the improvement of hardness of the coatings. Other mechanisms such as dispersion-strengthening (or *Orowan* strengthening) can also influence the hardness since the sizes of dispersed particles are comparable to the average nickel grain size (80–200 nm). Therefore, it is believed that the high hardness of the cermet coatings produced in this study is influenced by a combined effect of dispersion-strengthening of ceramic particles in the matrix as well as grain refinement of the matrix. Figure 9 provides a comparison between the microhardness for cermet coatings produced in this research as compared to reported values for several common cermet coatings reported by Low et al. [22]. The microhardness values for the produced cermet coatings in this research are imposed on the graph and show that their microhardness values are comparable to the reported values from other materials and coating production techniques.

4. Conclusion

Cermet coatings composed of one or two types of nanosized ceramic particles (α-Al_2O_3 and TiO_2) incorporated in a nickel matrix was successfully produced using a co-electrodeposition technique. The concentrations of particles in the standard *Watt*'s electrolyte solution were 0.25 and 0.5 mol and applied current densities of 1, 2 and 3 A/dm^2 were used. A uniform distribution of ceramic particles in the nickel matrix was observed for all coatings. Results showed that the volume fraction of dispersed particles in the matrix was increased when increasing the applied current density and concentration of particles in the electrolyte solution. For coatings composed of only α-Al_2O_3, a maximum particle deposition of 10.0% was obtained using an applied current density of 3 A/dm^2 and particle concentration of 0.5 M in electrolyte. For coatings composed of only TiO_2, a maximum particle deposition of 12.6% was obtained using an applied current density of 2 A/dm^2 and particle concentration of 0.5 M in electrolyte. For coatings composed of two types of ceramic particles a maximum particle deposition of 11.8% was achieved using a solution containing equal portions of ceramic in 0.5 M solutions (A1 coating) and under applied current density of 2 A/dm^2. The cermet coatings showed a higher hardness values compared to pure nickel coating under similar applied current density to a maximum microhardness of HV. 705 for Ni + Al_2O_3 coatings. It was found that the concentration of particles in the electrolyte has greater influence on the microhardness of coatings compared to applied current density. Coatings containing only α-Al_2O_3 particle dispersion showed greater hardness than coatings containing TiO_2 particles. The hardness of coatings composed of both α-Al_2O_3 and TiO_2 were found to correspond to the partial concentration of each ceramic particle in the electrolyte solution. The improvement in microhardness of the cermet coatings produced in this study was attributed to a combined effect of dispersion-strengthening of ceramic particles in the nickel matrix as well as grain refinement of the matrix.

Acknowledgement

The authors would like to thank the department of Mechanical and Manufacturing Engineering of the University of Calgary, Alberta, Canada, Natural Science and Engineering Research Council of Canada (NSERC), and Statoil Canada Ltd. for their financial support.

References

[1] Sautter FK. Electrodeposition of dispersion-hardened Nickel-Al_2O_3 Alloy. J. Electrochem. Soc. 1963;110:557–560.
[2] Gupta PK, Tiwari AN, Agrawal BK. Electrodeposition and mechanical properties of nickel-tungsten carbide composites. Trans. Jpn. Inst. Met. 1982;23:320–327.
[3] Saha RK, Haq IU, Khan TI, Glenesk LB. Development of wear resistant nano dispersed composite coating by electrodeposition. Key Eng. Mater. 2010;442:187–194.
[4] Saha RK, Khan TI, Glenesk LB, Haq IU. Formation of electrodeposition Ni–Al_2O_3 composite coating, processing of nanoparticle structures and composites. Ceram. Trans. 2009;208:37–44.
[5] Ciubotariu AC, Benea L, Varsanyi ML, Dragan V. Electrochemical impedance spectroscopy and corrosion behaviour of Al_2O_3–Ni nano composite. Electrochim. Acta. 2008;53: 4557–4563.
[6] Staia MH, Conzono A, Cruz MR, Roman A, Lesage J, Chicot D, Mesmacque G. Wear behaviour of silicon carbide/electroless nickel composite coatings at high temperatures. Surf. Eng. 2002;18:265–269.
[7] Szczygiel B, Kolodziej M. Composite Ni/Al_2O_3 coatings and their corrosion resistance. Electrochim. Acta. 2005;50:4188–4195.
[8] Saha RK, Khan TI. Effect of applied current on the electrodeposited Ni–Al_2O_3 composite coatings. Surf. Coat. Technol. 2010;205:890–895.
[9] Gül H, Kilic F, Aslan S, Alp A, Akbulut H. Charact. of electrocodeposited Ni–Al_2O_3 nanoparticle metal matrix composite coatings. Wear. 2009;267:976–990.
[10] Gabe DR. Principle of metal surface treatment and protection. 2nd ed. Vol. 28. Oxford: Pergamon; 1978.
[11] Erb U. Electrodeposited nanocrystals: synthesis, properties and industrial applications. NanoStrut. Mater. 1995;6:533–538.
[12] Bockris JO'M, Razumney G. A. Fundamental aspects of electrocrystallization. New York, NY: Plenum Press; 1967.
[13] Walsh FC, Herron ME. Electrocrystallization and electrochemical control of crystal growth: fundamental considerations and electrodeposition of metals. J. Phys. D: Appl. Phys. 1991;24:217–225.
[14] Qu NS, Chan KC, Zhu D. Pulse co-electrodeposition of nano Al_2O_3 whiskers nickel composite coating. Scr. Mater. 2004;50:1131–1134.
[15] Ruan S, Schuh CA. Mesoscale structure and segregation in electrodeposited nanocrystalline alloys. Scr. Mater. 2008;59:1218–1221.
[16] Feng Q, Li T, Teng H, Zhang X, Zhang Y, Liu Ch, Jin J. Investigation on the corrosion and oxidation resistance of Ni–Al_2O_3 nano-composite coatings prepared by sediment co-deposition. Surf. Coat. Technol. 2008;202:4137–4144.
[17] Kim MJ, Kim JS, Kim DJ, Kim HP. Electro-deposition of oxide-dispersed nickel composites and the behavior of their mechanical properties. Met. Mater. Int. 2009;15:789–795.
[18] Bund A, Thiemig D. Influence of bath composition and pH on the electrocodeposition of alumina nanoparticles and nickel. Surf. Coat. Technol. 2007;201:7092–7099.
[19] Thiemig D, Bund A. Characterization of electrodeposited Ni-TiO_2 nanocomposite coatings. Surf. Coat. Technol. 2008;202:2979–2984.
[20] Thiemig D, Bund A. Influence of ethanol on the electrocodeposition of Ni/Al_2O_3 nanocomposite films. Appl. Surf. Sci. 2009;255:4164–4170.
[21] Sadeghi A, Khosroshahia R, Sadeghian Z. Morphological, mechanical, corrosion and hydrogen permeation characteristics of Ni–nano–TiO2. J. Surf. Invest. 2011;5:186–192.
[22] Low C, Wills R, Walsh FC. Electrodeposition of composite coatings containing nanoparticles in a metal deposit. Surf. Coat. Technol. 2006;201:371–383.

[23] Sun XJ, Li JG. Friction and wear properties of electrodeposited nickel-titania nanocomposite coatings. Tribol Lett. 2007;28:223–228.
[24] Kuo SL, Chen YC, Ger MD, Hwu WH. Nano-particles dispersion effect on Ni/Al_2O_3 composite coatings. Mater. Chem. Phys. 2004;86:5–10.
[25] Marikkannu KR. Studies on nickel-alumina electrocomp. coat. of over steel substrate. Int'l Symposium Res. Studies on Material Science and Engineering; 2004 December 20–22, Chennai, India.
[26] Chen L, Wang L, Zeng Zh, Zhang J. Effect of surfactant on the electrodeposition and wear resistance of Ni–Al_2O_3 composite coatings. Mater. Sci. Eng., A. 2006;434:319–325.
[27] Thiemig D, Bund A, Talbot J. Influence of hydrodynamic & pulse plating parameters on electrocodeposition of nickel–alumina. Electrochim. Acta. 2009;54:2491–2498.
[28] Thiemig D, Bund A. Influence of ethanol on the electrocodeposition of Ni/Al_2O_3 nanocomposite films. Appl. Surf. Sci. 2009;255:4164–4170.
[29] Abdel Aal A, Hassan HB. Electrodeposited nanocomposite coatings for fuel cell application. J. Alloys Compd. 2009; 477:652–656.
[30] Spanou S, Pavlatou EA, Spyrellis N. Ni/nano-TiO_2 composite electrodeposits: textural and structural modifications. Electrochim. Acta. 2009;54:2547–2555.
[31] Parida G, Chaira D, Chopkar M, Basu A. Synthesis and characterization of Ni-TiO_2 coatings by electrocodeposition. Surf. Coat. Technol. 2011;205:4871–4879.
[32] Aruna ST, William Grips VK, Rajam KS. Synthesis and characterization Ni–Al_2O_3 composite coatings containing different alumina. J. Appl. Electrochem. 2010;40:2161–2169.
[33] Erler F, Jakob C, Romanus H, Spiess L, Wielage B, Lampke T, Steinhauser S. Interface behaviour in nickel composite coatings with nano-particles of oxidic ceramic. Electrochim. Acta. 2003;48:3063–3070.
[34] Aruna ST, William Grips VK, Ezhil Selvi V., Rajam KS. Studies on electrodeposited nickel–yttria doped ceria coatings. J. Appl. Electrochem. 2007;37:991–1000.
[35] Sen R, Bhattacharya S, Das S, Das K. Effect of surfactant on the co-electrodeposition of the nano-sized ceria particle in the nickel matrix. J. Alloys Compd. 2010;489:650–658.
[36] Srivastava M, et al. Electrochemical deposition and tribological behaviour of Ni and Ni–Co composites with SiC nanoparticles. Appl. Surf. Sci. 2007;253:3814–3824.
[37] Broutman LJ, Krock RH. Composite materials. Vol. 4, Metallic matrix composites. New York (NY): Academic Press; 1974.
[38] Callister WD. Materials science and engineering – an introduction. New York (NY): Wiley; 2003.
[39] Gawne DT, Gudyanga TFP. Wear behaviour of chromium electrodeposits, coatings and surface treatment for corrosion and wear resistance, Ellis, p. 28–45; 1984.
[40] Hultman L. Materials science of wear-protective nanostructured thin films. Vol. 155, NATO science series, Section II. Dordrecht: Kluwer Academic Publisher; 2004. p. 9–21.
[41] Bund A, Thiemig D. Influence of bath composition and pH on the electrocodeposition of alumina nanoparticles and copper. J. Appl. Electrochem. 2006;37:345–351.
[42] Zimmerman AF, Palumbo G, Aust KT, Erb U. Mechanical properties of nickel silicon carbide nanocomposites. Mater. Sci. Eng., A. 2002;328:137–146.
[43] Godon A. Effects of grain orientation on the Hall–Petch in electrodeposited nickel with nanocrystalline grains. Scr. Mater. 2010;62:403–406.
[44] Ebrahimi F. Mechanical properties of nanocrystalline nickel produced by electrodeposition. Nanostruct. Mater. 1999;11:343–350.
[45] El-Sherik AM, Shirokoff J, Erb U. Stress measurements in nanocrystalline Ni electrodeposits. J. Alloys Compd. 2005;389:140–143.
[46] El-Sherik A, Erb U, PalumboG, Aust KT. Deviations from Hall–Petch behaviour in as-prepared nanocrystalline nickel. Scrip. Metallu. Mat. 1992;27:1185–1188.
[47] Jeong DH, Gonzalez F, Palumbo G, Aust KT, Erb U. The effect of grain size on the wear properties of electrodeposited nanocrystalline nickel coatings. Scr. Mater. 2001;44:493–499.
[48] Alnegren P. Oxidation behavior of selected FeCr alloys in environments relevant for solid oxide electrolysis applications [M.Sc. Thesis]. Gothenburg, Sweden: Chalmers University of Technology; 2012.